

Fischer-Tropsch synthesis over unpromoted Co/ γ -Al₂O₃ catalyst: effect of activation with CO compared to H₂ on catalyst performance

Phathutshedzo R Khangale¹, Reinout Meijboom², Kalala Jalama^{1*}

¹ Department of Chemical Engineering, Faculty of Engineering and the Built Environment, University of Johannesburg, Doornfontein 2028, South Africa.

² Department of Chemistry, University of Johannesburg, P.O. Box 524, Auckland Park 2006, Johannesburg, South Africa

* Corresponding Author. E-mail: kjalama@uj.ac.za (K. Jalama),
Telp: +27-11-5596157, Fax: +27-11-5596159

Abstract

The effect of activating Co/Al₂O₃ catalyst by diluted CO or H₂ on catalyst performance for Fischer-Tropsch reaction was investigated. The catalyst was prepared by incipient wetness impregnation of the support and characterized using BET N₂ physisorption, SEM and XRD analyses. The reduction behavior of the catalyst in presence of CO and H₂ individually was evaluated using TPR analyses. The data reveal that CO activates Co/Al₂O₃ catalyst at a lower temperature than H₂ and produces a catalyst with higher rate for liquid product formation. It also leads to higher methane selectivity probably due to some cobalt carbide formation.

Keywords:

Co/Al₂O₃ catalyst; Fischer-Tropsch; Activation with CO.

1. Introduction

The activation of cobalt catalysts prior to FT reaction is an important step as it influences the catalyst performance. The major role of this process is to reduce cobalt species from oxidized form in the fresh catalyst into a metallic form that is active for FT reaction. This is usually achieved at high temperatures in presence of hydrogen [1]. During this process some cobalt species can interact with the support to form compounds that are difficult to reduce. For example in the case of alumina, the formation of cobalt-aluminate has been reported [2]. To improve the reducibility of cobalt-based catalysts, a number of techniques have been employed including catalyst promotion with a second

metal such as Pt [3], Ru [4], Re [5], Au [6], etc. The type of gas used to reduce cobalt catalysts can also affect the catalyst reducibility and performance for FT reaction. Earlier studies from our laboratory have reported positive effects in reducing 10% Co/TiO₂ catalyst using synthesis gas [7] and diluted CO [8]. The latter improved the catalyst activation, stability and the yield for C₅₊ hydrocarbons product at extended time on stream. The results have suggested that activating the catalyst with CO and H₂ separately leads to different types of interaction between cobalt and the TiO₂ support. The present work aims at extending this study to alumina-supported cobalt catalysts since no similar studies have been reported to date.

2. Experimental details

2.1 . Catalyst preparation and characterization

The catalyst was prepared by incipient wetness impregnation of the alumina support (from Sigma-Aldrich) using an aqueous solution of cobalt nitrate. After drying in air at 120 °C overnight, the sample was calcined in air at 500 °C for 10 hours.

The surface area and pore distribution for the support and the synthesized catalyst were determined by Brunauer-Emmett-Teller (BET) analyses that were performed on a Micromeritics Tristar 3000 using N₂. The samples were degassed under vacuum overnight at 90°C before N₂ adsorption. The total pore volume was determined using the amount of vapor adsorbed at a relative pressure. X-ray diffraction (XRD) analyses were used to determine the cobalt phase in the catalyst before and after reduction, and after the FT reaction following the procedure described in an earlier study [8]. Temperature programmed reduction (TPR) analyses were performed using a Micromeritics Autochem II apparatus to compare the catalyst behaviour during reduction in the presence of 10% H₂/Ar and 10% CO/He correspondingly. The calcined catalyst samples (100 mg) were initially loaded in a U-shaped quartz tube reactor and degassed using nitrogen gas (30 ml/min) at 150 °C for 30 min and cooled to room temperature. The sample was subsequently subjected to a continuous flow of the reducing gas mixture (30 ml/min) while the temperature was increased to 900 °C (10 °C/min). A thermal conductivity detector (TCD) was located at the reactor outlet to detect changes in H₂ or CO concentration in the analysis gas.

Scanning electron microscopy (SEM) analyses were performed using a Wigsam Tescan Vega 3 XMU apparatus to examine the catalyst morphology after reduction with CO or H₂.

2.2 Catalyst testing

The catalyst was evaluated for Fischer-Tropsch reaction in a fixed bed reactor constructed at the university. 0.5g of the catalyst was loaded in the reactor and various parameters such as the space velocity, pressure, temperature and effect of reducing gas mixture were evaluated. The catalyst was activated by reducing with either 5% H₂ in Ar or 5% CO in He for 17 hours to convert cobalt oxide to metallic cobalt since this is the active form for FT. The flow rate of the reducing gas mixture was set to 30 ml/min at atmospheric pressure. The temperature was elevated from room temperature to either 350 °C or 300 °C at a rate of 10 °C per minute and kept there for 17 hours.

FT runs were performed using syngas as a feed containing 10% N₂, 30% CO and 60% H₂. The outlet gas products was analysed using Dani master gas chromatograph (GC) equipped with thermal conductivity detector (TCD) and flame ionisation detector (FID). N₂ (10%) was present in the reaction feed as an internal standard used for accurate calculations of the CO conversion.

As N₂ was inert under FT conditions, its balance was written in Equation 1

$$\dot{n}_{T_{in}} \cdot \%N_{2_{in}} = \dot{n}_{T_{out}} \cdot \%N_{2_{out}} \dots\dots\dots(1)$$

Where $\dot{n}_{T_{in}}$ and $\dot{n}_{T_{out}}$ are the total molar flow rate in and out of the reactor and $\%N_{2_{in}}$ and $\%N_{2_{out}}$ are the percentage of N₂ flowing in and out respectively.

The %CO₂ conversion was calculated as follows:

$$\%CO \text{ conversion} = \frac{\dot{n}_{CO_{reacted}}}{\dot{n}_{CO_{in}}} \times 100\% = \frac{\dot{n}_{CO_{in}} - \dot{n}_{CO_{out}}}{\dot{n}_{CO_{in}}} \times 100\% \dots\dots\dots(2)$$

Where

$$\dot{n}_{CO_{in}} = \dot{n}_{T_{in}} \times \%CO_{in} \dots\dots\dots(3)$$

$$\dot{n}_{CO_{out}} = \dot{n}_{T_{out}} \times \%CO_{out} \dots\dots\dots(4)$$

$$\dot{n}_{T_{in}} \cdot \%N_{2_{in}} = \dot{n}_{T_{out}} \cdot \%N_{2_{out}} \dots\dots\dots(5)$$

$$\dot{n}_{T_{out}} = \dot{n}_{T_{in}} \cdot \frac{\%N_{2in}}{\%N_{2out}} \dots\dots\dots(6)$$

After substitution of equations 3 to 6 in equation 2, the % CO conversion was calculated as

$$\%CO \text{ conversion} = \frac{\%CO_{in} - \left(\frac{\%N_{2in}}{\%N_{2out}}\right) \cdot \%CO_{out}}{\%CO_{in}} \times 100\% \dots\dots\dots(7)$$

The rate of CO conversion was calculated as:

The rate of CH₄ production was calculated as:

$$r_{CH_4} = \dot{n}_{T_{out}} \cdot \frac{\%CH_{4out}}{100} \dots\dots\dots(8)$$

The selectivity of CH₄ was expressed as follows:

$$CH_4 \text{ selectivity} = \frac{r_{CH_4}}{-r_{CO}} \times 100\% \dots\dots\dots(9)$$

The selectivity of C₂-C₄ was calculated using the following expression

$$C_n \text{ selectivity} = \frac{[(r_{C_nH_{n+1}} + r_{C_nH_{n+2}}) \times n]}{-r_{CO}} \times 100\% \dots\dots\dots(10)$$

Where n is the number of carbons (positive integer 2, 3 or 4)

The selectivity of C₅₊ was calculated as follows:

$$C_{5+} \text{ selectivity} = 100\% - CH_4 \text{ selectivity} - \sum (C_2 + C_3 + C_4) \text{ selectivity} \dots\dots\dots(11)$$

3. Results and Discussion

3.1. Catalyst characterization

BET analysis data for the blank calcined γ -Al₂O₃ support and the fresh calcined Co/Al₂O₃ catalyst are reported in Table 1.

Table 1
Summary for BET analysis data

	Calcined blank Al ₂ O ₃ support	Calcined 15 %Co/Al ₂ O ₃ catalyst
BET surface area [m ² /g]	123.6	110.0
Pore Volume [cm ³ /g]	0.229	0.193
Pore size [nm]	56.2	62.0

The BET surface area and the total pore volume for the calcined Co/ γ -Al₂O₃ catalyst were 110 m²/g and 0.193 cm³/g respectively. These values were lower than those for the blank γ -Al₂O₃ support which had a surface area of 123.6 m²/g and pore volume of 0.229 cm³/g. The decrease in surface area and pore volume after addition of cobalt to the support was possibly due to some pore obstruction by cobalt species deposited inside the pores of the γ -Al₂O₃ support. The increase in pore size from 56.2 nm in the blank support to 62 nm in the calcined catalyst could suggest that some pores possibly collapsed during the second calcination process used to decompose the added cobalt nitrate to the support.

TPR analyses data are reported in Fig. 1.

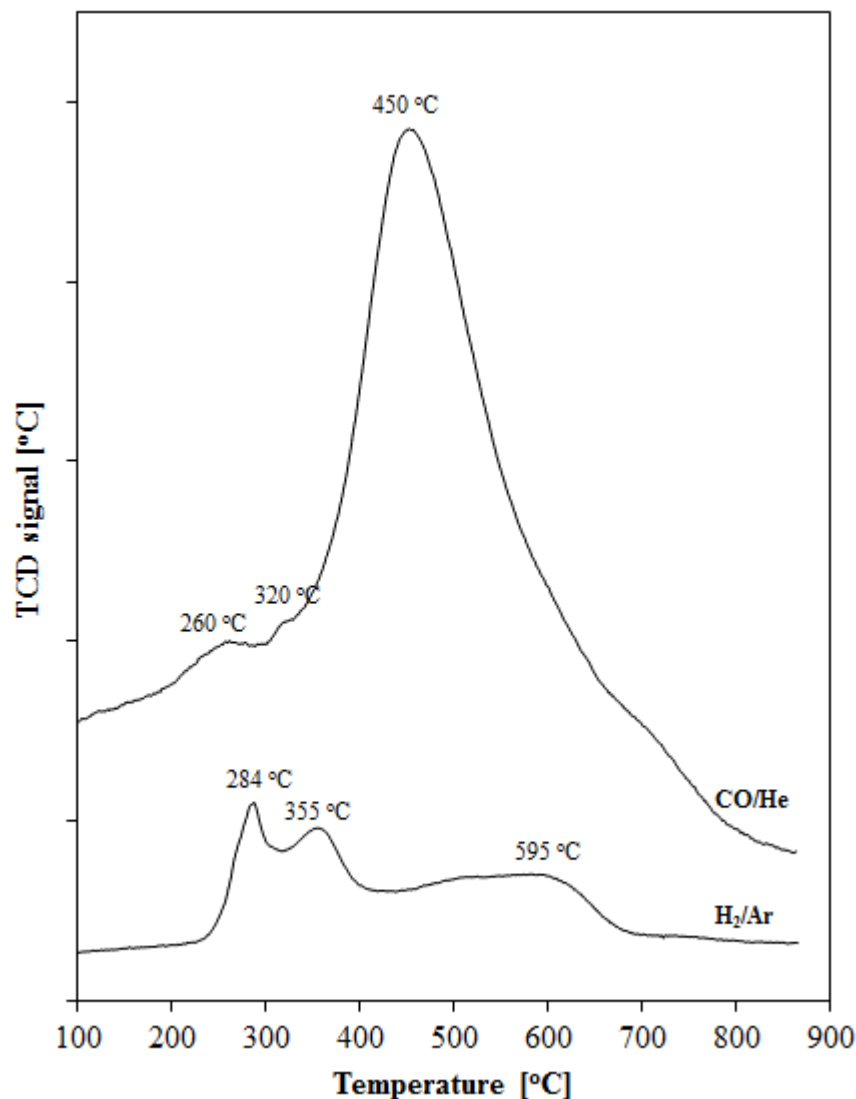


Fig. 1. TPR profiles for catalyst samples in presence of CO/He and H₂/Ar.

When Co/Al₂O₃ catalyst reduction was conducted with CO/He, the first peak reached its maximum at ca. 260 °C. This peak was followed by a second peak with a maximum at ca. 320 °C before observing a large peak that started at ca. 330 °C, reached a maximum at 450 °C and extended to 850 °C. The first two peaks were respectively attributed to the two-step reduction of cobalt oxide species to CoO and Co⁰. The large peak with maximum at 450 °C was due to carbon deposition on the catalyst sample. Carbon deposition during cobalt catalyst reduction by diluted CO (10 vol.%) was also observed in a similar temperature range (between 315 and 415 °C) on a Co/ZnO catalyst by Pan and Bukur [9]. It happened at higher temperatures, i.e. ca. 480 °C on bulk Co₃O₄ and 560 °C on Co/TiO₂ catalyst in

presence of 5% CO [8].

The first peak for the Co/Al₂O₃ sample in presence of 10% H₂/Ar started at ca. 225 °C with its maximum at 284 °C and was attributed to the first step reduction of Co₃O₄ species to CoO. The second peak with a maximum at 355 °C was attributed to the reduction of CoO to Co⁰ and was followed by an extended peak from ca. 400 to 680 °C attributed to the reduction of cobalt species in strong interaction with the Al₂O₃ support [10].

In agreement with earlier studies [7 - 9] the data in Fig. 1 show that cobalt catalyst reduction using CO occurs at lower temperatures compared to the reduction using H₂. This suggests that CO improves catalyst reduction.

Fig. 2 shows SEM images for catalyst samples after reduction by CO and H₂ respectively.

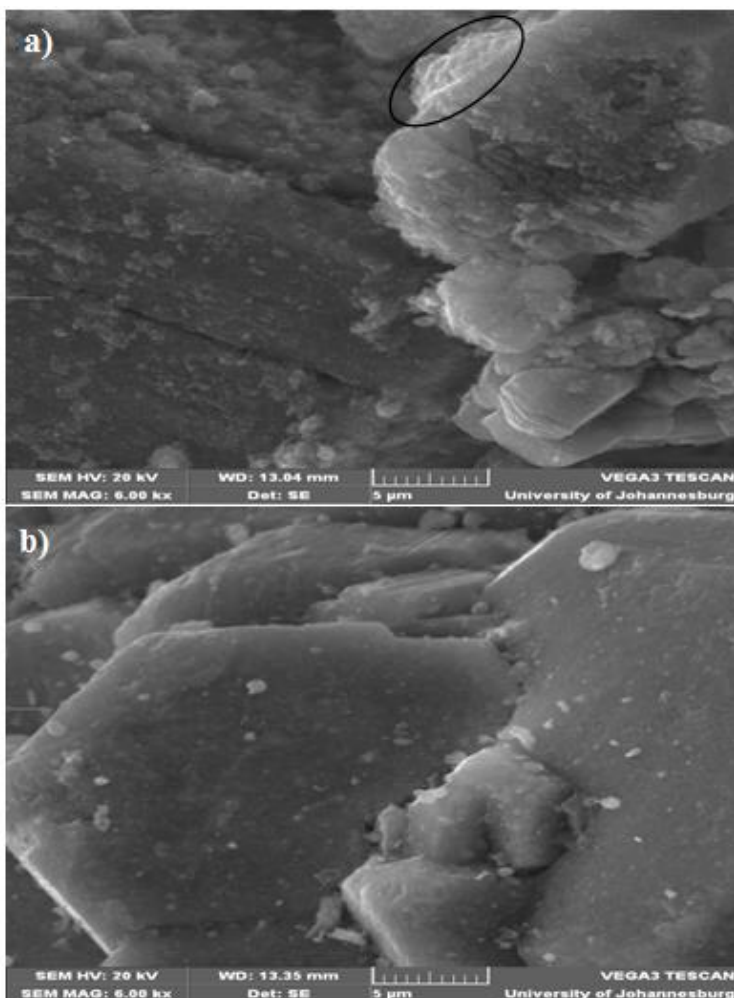


Fig. 2. SEM micrographs for a) CO- reduced catalyst at 350 °C, b) H₂ -reduced catalyst at 350 °C.

The micrographs show some level of coverage of CO-reduced catalyst samples (Fig. 2a) by some amorphous materials. These materials are not observed on H₂-reduced catalyst samples (Fig. 2b) and are believed to be deposited carbon.

XRD analysis data for the catalyst before and after activation using CO and H₂ at 350 °C are reported in Fig. 3.

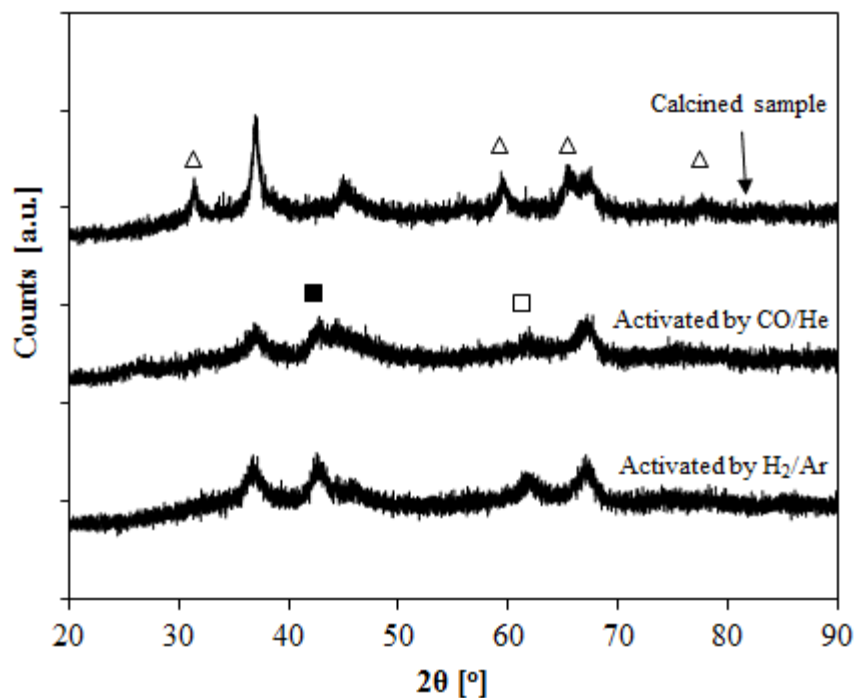


Fig. 3. XRD data for calcined catalyst samples before activation, after activation by CO and after activation by H₂ at 350 °C (Δ Co₃O₄, ■ CoO, □ Co⁰).

Cobalt was present as Co₃O₄ in the calcined catalyst. Diffraction peaks for CoO and Co⁰ were detected in both CO- and H₂-activated catalyst samples. However the diffraction peak for Co⁰ in the CO-activated sample appeared less intense and broader compared to the H₂-activated catalyst. This could suggest that cobalt was more dispersed on the support after activation by CO.

Fig. 4 shows XRD data for catalyst samples (activated by CO or H₂ at 350 °C) after FT reaction. The data reveal the presence of cobalt carbide on the CO-reduced catalyst and not on the H₂-reduced catalyst.

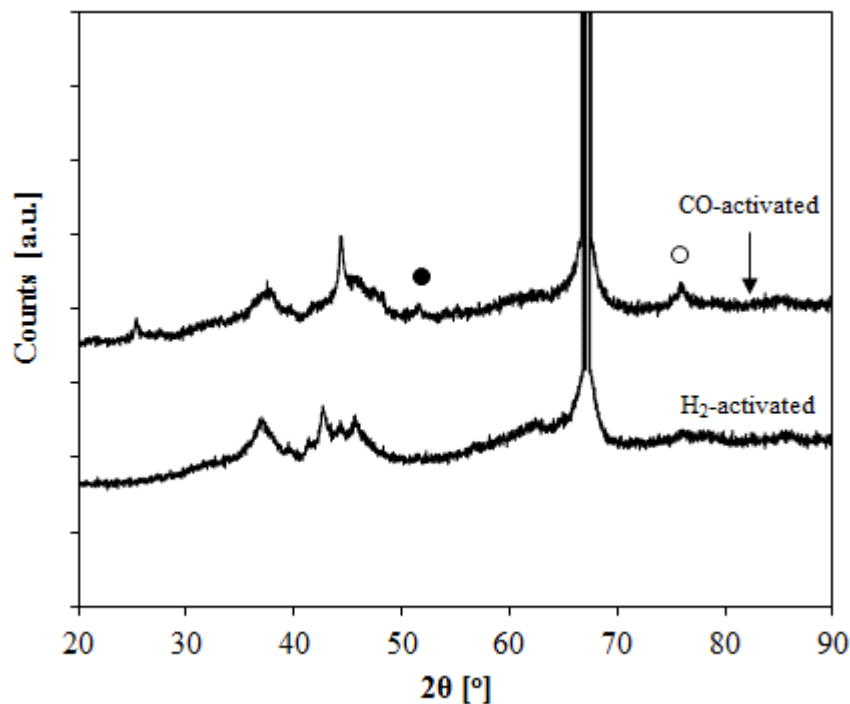


Fig. 4. XRD data for catalyst samples after FT reaction (● Co_3C , ○ Co_2C).

3.2. Catalyst evaluation

Catalyst evaluation data are summarized in Table 2. Under similar operating conditions, the catalyst samples that were respectively reduced at 300 and 350 °C by H_2 showed comparable performance for FT reaction with CO conversions around 11 – 12% and methane selectivity between 3 and 6%. C_3 – C_5 olefin to paraffin ratios were also similar.

Increasing the space velocity for the H_2 -reduced catalyst decreased the CO conversion, as expected, due to the short reactants residence time in the reactor and increased the rate for product formation ($r_{\text{C}_{5+}}$) and the C_3 - C_4 olefin to paraffin ratios. The space velocity did not seem to influence the methane selectivity as it fluctuated around 6%. The increase in product formation rate with an increase in space velocity can be explained by higher liquid hydrocarbons removal rate from the catalyst [11].

The effects of space velocity on CO conversion and C_{5+} product formation rate over the CO-reduced catalyst sample were similar to those observed for H_2 -reduced catalysts samples. However, the methane selectivity decreased and the selectivity for C_{5+} product increased as the space velocity was increased. No consistent correlation between olefin to paraffin ratios and the space velocity was obtained. The methane selectivity change as function of space velocity observed in this study seems

to differ from previous studies [12 - 15] which observed an opposite trend over alumina-supported cobalt catalysts reduced by H₂. This could suggest that catalyst pre-treatment with CO leads to different active sites distribution in the catalyst. When reduced at lower temperature, i.e. 300 °C by CO, the catalyst showed lower CO conversion and methane selectivity, and higher C₃ – C₅ olefin to paraffin ratio compared to the corresponding conditions for the catalyst reduced at 350 °C. When compared at similar operating conditions, CO-reduced catalysts displayed higher CO conversions and methane selectivity, and a higher rate of liquid product (rC₅₊) formation compared to H₂-reduced samples. For example, ca. 15% CO conversion, 8.3% CH₄ selectivity and a rC₅₊ of ca. 2.9 g/gCat/h were obtained for the catalyst sample reduced at 300 °C by CO compared to respective values of ca. 12% CO conversion, 3.3% CH₄ selectivity and rC₅₊ of ca. 2.4 g/gCat/h for the catalyst sample reduced at the same temperature by H₂

Table 2
Summary of FT reaction data

Reducing gas	SV [L/gCat/h]	Red. Temp [°C]	CO conv. [%]	Selectivity [%]			O/P ratio						rC ₅₊ [g/gCat/h]
				CH ₄	C ₂ - C ₄	C ₅₊	C ₂	C ₃	C ₄	C ₅	C ₆	C ₇	
5% H ₂ /Ar	1.2	300	11.58	3.3	0.84	95.86	0.01	2.39	2.23	0.8	0.43	0.29	2.369
	0.2	350	13.69	5.7	1.17	93.13	0.35	1.46	0.97	0.34	0.57	0.17	0.546
	0.8	350	12.23	6.6	0.67	92.73	0.47	1.84	1.06	0.76	0.31	0	1.692
	1.2	350	11.98	5.7	0.84	93.46	0.39	2.04	2.19	0.63	0	0	2.39
5%CO/He	1.2	300	14.85	8.3	21.50	70.20	0	1.44	2.32	1.35	1.06	0.66	2.874
	0.2	350	33.05	27.9	11.18	60.92	0.74	1.21	1.28	0.76	0.56	0.44	1.006
	0.8	350	24.76	16.9	10.14	72.96	0.6	1.36	1.11	0.79	0.48	0.33	3.042
	1.2	350	18.81	15.0	6.45	78.55	0.74	1.35	1.09	0.76	0.67	0.32	3.38

The high activity for the CO-reduced catalyst could be due to better catalyst reduction as suggested by TPR data discussed in Section 3.1. Higher methane selectivity for CO-reduced catalysts is usually explained by the presence of cobalt carbides in the catalyst [9, 16, 17]. As shown by XRD data in Section 3.1, no cobalt carbide was detected in CO-reduced catalyst sample before FT reaction but was found in used catalyst (Fig. 4). This indicates that it had formed during FT reaction and most probably during reaction start-up as the partial pressure of CO was increased. The latter assumption can be supported by the fact that no significant change in catalyst activity and methane selectivity was observed during normal FT run. Also, cobalt carbides are usually associated with low FT catalyst activities [9, 17] but surprisingly in this study, high activities have been measured on CO-reduced catalyst on which cobalt carbides formed. This suggests that the formation of cobalt carbides and their role during FT reaction are strongly influenced by the catalyst structure and the type of cobalt interaction with the support. The following examples from literature can support this assumption: i) under similar testing conditions Co_2C were reported to form on TiO_2 - and Al_2O_3 -supported Co catalyst during CO hydrogenation but not on SiO_2 -supported catalysts [18]; ii) more cobalt carbide formed during FT reaction over a $\text{CoPt}/\text{Al}_2\text{O}_3$ catalyst which was calcined at 500 °C compared to that calcined at 300 °C [19]; iii) no activity was measured on carburized Pt-promoted alumina-supported cobalt catalysts and the cobalt carbide was stable under realistic FT conditions [19]. However, the opposite was observed for bulk Co_2C [16] and carburized 10%Co/ TiO_2 [17] which showed some initial low FT activity and were converted to a more metallic form as the FT reaction progressed.

The formation of cobalt carbides in CO-reduced catalyst during FT reaction, as observed in this study, suggests that catalyst activation with CO and H_2 respectively leads to different types of cobalt interaction with the support which in turn produce a different distribution of active sites in the catalyst. The high activity measured on CO-reduced catalyst in spite of cobalt carbide formation during FT reaction indicates that catalyst reduction by CO produced a higher number of active sites in the catalyst compared to reduction with H_2 . Part of these sites were carburized upon exposure to high-pressure CO during the start of FT reaction and increased the methane selectivity.

4 Conclusions

TPR data have revealed that CO activates $\text{Co}/\text{Al}_2\text{O}_3$ catalyst at a lower temperature than H_2 . The main form of cobalt species in catalyst samples reduced by CO or H_2 at 350 °C was CoO and Co^0 . Cobalt carbides were not detected in the reduced catalyst samples but formed during FT reaction on CO-reduced catalyst and explained the higher methane selectivity measured on this catalyst. The

CO-reduced catalyst displayed more activity and higher rate for liquid product formation during FT reaction. The results suggest that reducing cobalt catalyst by CO or H₂ leads to different types of cobalt interaction with the alumina support.

Acknowledgment

Financial support from the National Research Foundation (NRF) and the University of Johannesburg is hereby acknowledged.

References

- [1] Steynberg, A. P. (2004). Introduction to fischer-tropsch technology. *In Studies in surface science and catalysis*, 152: 1-63.
- [2] Zhang, Y., Wei, D., Hammache, S., Goodwin Jr, J. G. (1999). Effect of water vapor on the reduction of Ru-promoted Co/Al₂O₃. *Journal of Catalysis*, 188(2): 281-290.
- [3] Zsoldos, Z., Guzzi, L. (1992). Structure and catalytic activity of alumina supported platinum-cobalt bimetallic catalysts. 3. Effect of treatment on the interface layer. *The Journal of Physical Chemistry*, 96(23): 9393-9400..
- [4] Kogelbauer, A., Goodwin Jr, J. G., Oukaci, R. (1996). Ruthenium Promotion of Co/Al₂O₃Fischer–Tropsch Catalysts. *Journal of Catalysis*, 160(1): 125-133.
- [5] Das, T. K., Jacobs, G., Patterson, P. M., Conner, W. A., Li, J., Davis, B. H. (2003). Fischer–Tropsch synthesis: characterization and catalytic properties of rhenium promoted cobalt alumina catalysts. *Fuel*, 82(7): 805-815.
- [6] Jalama, K., Coville, N. J., Xiong, H., Hildebrandt, D., Glasser, D., Taylor, S., Hutchings, G. J. (2011). A comparison of Au/Co/Al₂O₃ and Au/Co/SiO₂ catalysts in the Fischer–Tropsch reaction. *Applied Catalysis A: General*, 395(1-2): 1-9.
- [7] Jalama, K., Kabuba, J., Xiong, H., Jewell, L. L. (2012). Co/TiO₂ Fischer–Tropsch catalyst activation by synthesis gas. *Catalysis Communications*, 17: 154-159.
- [8] Jalama, K. (2016). Fischer–Tropsch synthesis over Co/TiO₂ catalyst: Effect of catalyst activation by CO compared to H₂. *Catalysis Communications*, 74: 71-74.
- [9] Pan, Z., Bukur, D. B. (2011). Fischer–Tropsch synthesis on Co/ZnO catalyst—Effect of pretreatment procedure. *Applied Catalysis A: General*, 404(1-2): 74-80.
- [10] Jacobs, G., Das, T. K., Zhang, Y., Li, J., Racoillet, G., Davis, B. H. (2002). Fischer–Tropsch synthesis: support, loading, and promoter effects on the reducibility of cobalt catalysts. *Applied Catalysis A: General*, 233(1-2): 263-281.

- [11] Liu, Y., Edouard, D., Nguyen, L. D., Begin, D., Nguyen, P., Pham, C., & Pham-Huu, C. (2013). High performance structured platelet milli-reactor filled with supported cobalt open cell SiC foam catalyst for the Fischer–Tropsch synthesis. *Chemical engineering journal*, 222: 265-273.
- [12] Storsæter, S., Borg, Ø., Blekkan, E. A., Holmen, A. (2005). Study of the effect of water on Fischer–Tropsch synthesis over supported cobalt catalysts. *Journal of Catalysis*, 231(2): 405-419.
- [13] Borg, Ø., Eri, S., Blekkan, E. A., Storsæter, S., Wigum, H., Rytter, E., Holmen, A. (2007). Fischer–Tropsch synthesis over γ -alumina-supported cobalt catalysts: effect of support variables. *Journal of Catalysis*, 248(1): 89-100.
- [14] Ma, W., Jacobs, G., Ji, Y., Bhatelia, T., Bukur, D. B., Khalid, S., Davis, B. H. (2011). Fischer–Tropsch synthesis: Influence of CO conversion on selectivities, H₂/CO usage ratios, and catalyst stability for a Ru promoted Co/Al₂O₃ catalyst using a slurry phase reactor. *Topics in Catalysis*, 54(13-15): 757.
- [15] Ma, W., Jacobs, G., Keogh, R. A., Bukur, D. B., Davis, B. H. (2012). Fischer–Tropsch synthesis: Effect of Pd, Pt, Re, and Ru noble metal promoters on the activity and selectivity of a 25% Co/Al₂O₃ catalyst. *Applied Catalysis A: General*, 437: 1-9.
- [16] Mohandas, J. C., Gnanamani, M. K., Jacobs, G., Ma, W., Ji, Y., Khalid, S., Davis, B. H. (2011). Fischer–Tropsch synthesis: characterization and reaction testing of cobalt carbide. *ACS Catalysis*, 1(11): 1581-1588.
- [17] Yang, J., Jacobs, G., Jermwongratanachai, T., Pendyala, V. R. R., Ma, W., Chen, D., Davis, B. H. (2014). Fischer–Tropsch synthesis: impact of H₂ or CO activation on methane selectivity. *Catalysis letters*, 144(1): 123-132.
- [18] Ducreux, O., Rebours, B., Lynch, J., Roy-Auberger, M., Bazin, D. (2009). Microstructure of supported cobalt Fischer-Tropsch catalysts. *Oil & Gas Science and Technology-Revue de l'IFP*, 64(1): 49-62.
- [19] Karaca, H., Safonova, O. V., Chambrey, S., Fongarland, P., Roussel, P., Griboval-Constant, A., Khodakov, A. Y. (2011). Structure and catalytic performance of Pt-promoted alumina-supported cobalt catalysts under realistic conditions of Fischer–Tropsch synthesis. *Journal of catalysis*, 277(1): 14-26.
- [20] Moyo, M., Motchelaho, M. A., Xiong, H., Jewell, L. L., Coville, N. J. (2012). Promotion of Co/carbon sphere Fischer–Tropsch catalysts by residual K and Mn from carbon oxidation by KMnO₄. *Applied Catalysis A: General*, 413: 223-229.